Modern radio engineering and telecommunication systems

Современные радиотехнические и телекоммуникационные системы

UDC 621.314:681.586.7:004.942
https://doi.org/10.32362/2500-316X-2024-12-1-69-79

RESEARCH ARTICLE

Mathematical model of a DC/DC converter based on SEPIC topology

Aleksey I. Lavrenov @, Vladimir K. Bityukov

MIREA – Russian Technological University, Moscow, 119454 Russia
@ Corresponding author, e-mail: lavrenov@mirea.ru

Abstract

Objectives. A DC/DC converter based on SEPIC topology is a unipolar electronic device which converts an input positive voltage into a stabilized output voltage of the same polarity. It also has the ability to regulate polarity both below and above the input voltage. The aim of the paper is to analyze the DC/DC converter in its both operation phases, as well as to draw up equivalent circuits and obtain characterizing differential equations using Kirchhoff's rules for each phase. Each system of differential equations is reduced to Cauchy equations, in order to be further transformed into a limiting continuous mathematical model. Each system of equations is converted into a matrix form and subsequently combined into a single matrix system.

Methods. The construction of a limiting continuous mathematical model was accomplished using Kirchhoff's rules. *Multisim* software was used for the computer simulation, thus enabling the calculated results of direct currents and voltages to be compared to those of the simulation.

Results. Results show that the phase coordinates of the mathematical model tend towards the values of real currents and voltages of the converter at a switching frequency higher than 200 kHz. Fairly good agreement is established between the calculated values of currents and voltages and the values obtained by simulation (with varying fill factor and switching frequency).

Conclusions. The resulting limiting continuous mathematical model of the DC/DC converter based on SEPIC topology allows for an estimation of the dependence of the currents flowing through the inductor windings and the voltages across the capacitors on a number of parameters. The limiting continuous mathematical model of the DC/DC converter based on SEPIC topology is the basis for its circuit design and physical-and-mathematical analysis.

Keywords: DC/DC converter, buck-boost converter, equivalent circuit, SEPIC topology, limiting continuous mathematical model, Kirchhoff's rules, system of differential equations, Cauchy form, simulation

• **Submitted:** 09.04.2023 • **Revised:** 06.05.2023 • **Accepted:** 31.11.2023

For citation: Lavrenov A.I., Bityukov V.K. Mathematical model of a DC/DC converter based on SEPIC topology. *Russ. Technol. J.* 2024;12(1):69–79. https://doi.org/10.32362/2500-316X-2024-12-1-69-79

Financial disclosure: The authors have no a financial or property interest in any material or method mentioned.

The authors declare no conflicts of interest.

НАУЧНАЯ СТАТЬЯ

Математическая модель DC/DC-преобразователя, построенного по топологии SEPIC

А.И. Лавренов @**,**
В.К. Битюков

МИРЭА – Российский технологический университет, Москва, 119454 Россия
@ *Автор для переписки, e-mail: lavrenov@mirea.ru*

Резюме
Цели. DC/DC-преобразователь, построенный по топологии SEPIC, является униполярным электронным устройством, которое обеспечивает преобразование входного положительного напряжения в стабилизированное выходное напряжение той же полярности с возможностью его регулирования как ниже входного напряжения, так и выше. Цель статьи – выполнить анализ DC/DC-преобразователя в обеих фазах его работы. Для каждой из фаз необходимо составить эквивалентные схемы и получить характеризующие дифференциальные уравнения с помощью правил Кирхгофа. Каждую систему дифференциальных уравнений нужно привести к виду Коши для дальнейшего преобразования в предельную непрерывную математическую модель, а каждую систему уравнений преобразовать в матричный вид и впоследствии объединить в единую матричную систему.
Методы. Задача построения предельной непрерывной математической модели решена с использованием правил Кирхгофа. Для компьютерного моделирования была применена программа *Multisim*. Это позволило сопоставить результаты расчета постоянных токов и напряжений и моделирования.
Результаты. Показано, что фазовые координаты математической модели стремятся к значениям реальных токов и напряжений преобразователя при частоте коммутации силового ключа более 200 кГц. Установлено достаточно хорошее соответствие расчетных значений токов и напряжений и их значений, полученных с помощью моделирования (при вариации коэффициента заполнения и частоты коммутации).
Выводы. Полученная предельная непрерывная математическая модель DC/DC-преобразователя, построенного по топологии SEPIC, позволяет оценить зависимость токов, протекающих через обмотки дросселей, и напряжения на конденсаторах от ряда параметров. Предельная непрерывная математическая модель DC/DC-преобразователя, построенного по топологии SEPIC, является базой его схемотехнического проектирования и физико-математического анализа.

Ключевые слова. DC/DC-преобразователь, понижающе-повышающий преобразователь, эквивалентная схема, топология SEPIC, предельная непрерывная математическая модель, правила Кирхгофа, система дифференциальных уравнений, форма Коши, моделирование

• **Поступила:** 09.04.2023 • **Доработана:** 06.05.2023 • **Принята к опубликованию:** 31.11.2023

Для цитирования: Лавренов А.И., Битюков В.К. Математическая модель DC/DC-преобразователя, построенного по топологии SEPIC. *Russ. Technol. J.* 2024;12(1):69−79. https://doi.org/10.32362/2500-316X-2024-12-1-69-79

Прозрачность финансовой деятельности: Авторы не имеют финансовой заинтересованности в представленных материалах или методах.

Авторы заявляют об отсутствии конфликта интересов.

INTRODUCTION

A feature of the construction of a modern radio-electronic device is the transition from mains power to autonomous power supply. This is characteristic of knowledge-intensive devices in many spheres of life such as communication devices, personal computers, measuring devices, and others. Autonomous devices are traditionally used in broad applications in aviation, medicine and space technology. The primary energy sources in these areas are lithium-ion batteries, rechargeable batteries, fuel cells, solar cells, and others [1–3]. Each of these power sources generates a voltage which is highly time-varying, hence the need for DC/DC converters in power supply devices [4]. Most DC/DC converters offered by electronic component manufacturers are either step-up, step-down, or polar-inverting. Only a small number combine the functions of increasing and decreasing output voltage relative to the input voltage and its stabilization [5, 6].

Efficient buck-boost DC/DC converters are devices built according to SEPIC, Cuck, and Zeta topologies [7]. The high efficiency rate of converters and the stability of their output voltage, as well as the need for small mass-size parameters predetermine the strict requirements for the design of such converters. An integrated approach to design may be achieved by applying the limiting continuous mathematical model (LCM) of DC/DC converter, circuit simulation, and experimental study.

The mathematical derivation and description of the technology of building LCM with periodic high-frequency structure change are presented in [8, 9]. In [10–12], examples of using this technology on basic step-up, step-down, and inverting converters, as well as the analysis of their LCMs are given. In [13, 14], the LCM of a buck-boost converter based on Cuck topology is indicated. The limiting continuous models under consideration here are systems whose phase trajectories are continuous, i.e. characteristic of real technical devices. The limiting nature of the system consists in the fact that when the period decreases, the accuracy of the phase trajectories of the system describes the properties of the modeled object to a greater extent.

The first developed and investigated LCM for Zeta DC/DC converter is proposed in [15, 16]. Analytical equations which determine and analyze Zeta converter ripples are presented in [17].

Unfortunately, a LCM for SEPIC converter has not yet been developed, so the aim of the paper is to develop and investigate this.

CIRCUIT ENGINEERING

The SEPIC, Cuck, and Zeta topologies of buck-boost DC/DC converters are accomplished almost using the same electronic component base. However, they have their own features due to differences in switching [18].

In the operation of SEPIC DC/DC converters (Fig. 1), as well as in other converters, there are two phases of operation traditionally determined by the state of the power transistor VT1 [19].

The first phase of the SEPIC converter operation is accomplished with transistor VT1 fully open. This is referred to as the accumulation phase. In this phase, energy is accumulated in the magnetic field of inductors L1 and L2, with inductor L1 accumulating energy in the form of an electromagnetic field from the input current flowing through the inductor winding, and inductor L2 accumulating energy from the voltage across capacitor C1. During this phase, capacitor C2 discharges to the load, thus forming the output voltage U_{out}.

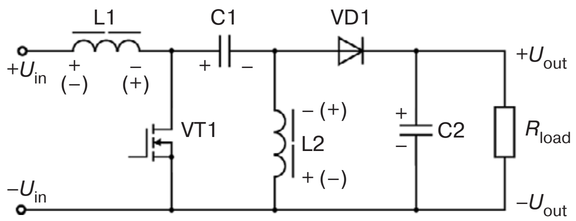

Fig. 1. Schematic circuit diagram of a buck-boost DC/DC converter based on SEPIC topology. U_{in} is the converter input voltage, R_{load} is the resistance. Here and in the following figures, the designations of circuit elements correspond to the designations adopted in GOST 2.710-81[1]

The second phase of the SEPIC converter operation is accomplished with the power transistor VT1 closed and is referred to as the discharge phase. The energy accumulated in the magnetic field of inductors L1 and L2 is used for charging capacitors C1 and C2.

MATHEMATICAL MODEL

Developing LCM for SEPIC converter requires describing each phase of the converter operation in terms of systems of differential equations in Cauchy form. It would be reasonable also to use Kirchhoff's rules to write these systems of equations. In order for the circuit equations of each phase of DC/DC converter operation to integrate alternating currents flowing through the windings of inductors L1 and L2, the inductors need to be represented in the form of series connected resistors R1 and R2 characterizing the ohmic resistance of the inductors and inductances L1 and L2.

The equivalent circuit of the first phase of the converter operation is shown in Fig. 2. Here the input power supply is labeled as E, while the inductors are represented as equivalent circuits. As can be seen from Fig. 2, all nodes of the circuit are connected to each other by conductors only, so they can be combined into one node.

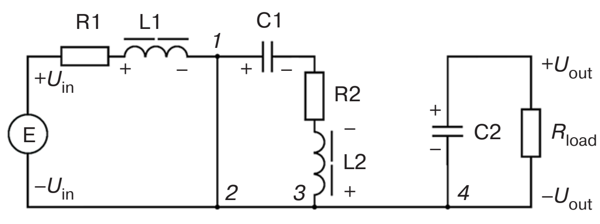

Fig. 2. Equivalent circuit of SEPIC converter operating in the energy accumulation phase

The equivalent circuit of the second phase of the converter operation is shown in Fig. 3, demonstrating

[1] GOST 2.710-81. *Interstate Standard. Unified system for design documentation. Alpha-numerical designations in electrical diagrams*. Moscow: Izd. Standartov; 1985 (in Russ.).

that nodes *1*, *3* and *2*, *4* are also connected to each other by conductors only. They can thus be combined into two nodes in pairs. It would be reasonable to combine the nodes in the circuits shown in Figs. 2 and 3, and designate contours on them (Figs. 4 and 5). Using the contours and nodes shown in Figs. 4 and 5, the equations of currents and voltages based on Kirchhoff's laws can be written.

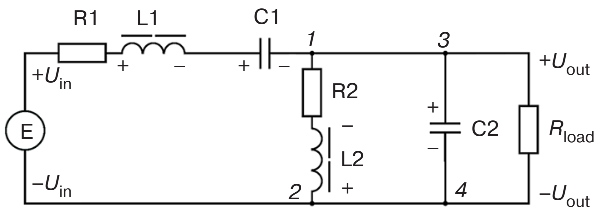

Fig. 3. Equivalent circuit of SEPIC converter operating in the energy transfer phase

First phase

The circuit shown in Fig. 4 has three branches and one node. Therefore, according to Kirchhoff's laws, the system of differential equations describing the first phase of DC/DC converter operation consists of three equations based on Kirchhoff's second law.

For circuits K1, K2, and K3 (Fig. 4), the following voltage equations can be written:

$$U_{\text{in}} = r_1 i_{\text{L1}} + L_1 \frac{di_{\text{L1}}}{dt}, \quad (1)$$

$$0 = -u_{\text{C1}} - r_2 i_{\text{L2}} - L_2 \frac{di_{\text{L2}}}{dt}, \quad (2)$$

$$0 = R_{\text{load}} i_{\text{load}} - u_{\text{C2}}, \quad (3)$$

where L_1 and L_2 are inductances of inductors; i_{L1} and i_{L2} are currents flowing through the windings of inductors L1 and L2; r_1 and r_2 are ohmic resistances of inductor windings L1 and L2; u_{C1} and u_{C2} are voltages on capacitors C1 and C2; and i_{load} is current flowing through the load with resistance R_{load}; U_{in} is the converter input voltage.

For the first phase, the currents flowing through capacitors C1 and C2 are defined by the following formulas:

$$i_{\text{L2}} = C_1 \frac{du_{\text{C1}}}{dt}, \quad (4)$$

$$i_{\text{load}} = C_2 \frac{du_{\text{C2}}}{dt}, \quad (5)$$

where C_1 and C_2 are capacitance of capacitors.

By expressing $\frac{di_{\text{L1}}}{dt}$ from Eq. (1), $\frac{di_{\text{L2}}}{dt}$ from Eq. (2), and $\frac{du_{\text{C1}}}{dt}$ from Eq. (4), the first three equations in Cauchy form are obtained. Substituting the load current from Eq. (5) into Eq. (3), we express $\frac{du_{\text{C2}}}{dt}$, thereby obtaining another equation in Cauchy form, as follows:

$$\begin{cases} \dfrac{di_{\text{L1}}}{dt} = \dfrac{U_{\text{in}}}{L_1} - \dfrac{r_1}{L_1} i_{\text{L1}}, \\ \dfrac{di_{\text{L2}}}{dt} = -\dfrac{1}{L_2} u_{\text{C1}} - \dfrac{r_2}{L_2} i_{\text{L2}}, \\ \dfrac{du_{\text{C1}}}{dt} = \dfrac{1}{C_1} i_{\text{L2}}, \\ \dfrac{du_{\text{C2}}}{dt} = \dfrac{1}{R_{\text{load}} C_2} u_{\text{C2}}. \end{cases} \quad (6)$$

Thus, Eqs. (6) form a system of differential equations in Cauchy form (6) describing the first phase of the SEPIC DC/DC converter operation.

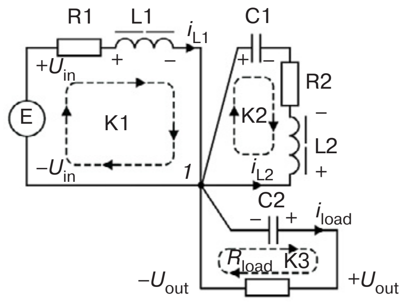

Fig. 4. Contours on the SEPIC converter circuit operating in the energy accumulation phase

Second phase

The circuit shown in Fig. 5 has four branches and two nodes. Therefore, according to Kirchhoff's rules, the system of differential equations describing the second phase of the converter consists of one equation based on Kirchhoff's first rule, and three equations based on the second rule. For node *1*, the following equation of currents can be written:

$$i_{\text{load}} = i_{\text{L1}} + i_{\text{L2}} - i_{\text{C2}}. \quad (7)$$

For circuits K1, K2, and K3, voltage equations in the following form can be written:

$$U_{\text{in}} = r_1 i_{\text{L1}} + L_1 \frac{di_{\text{L1}}}{dt} - u_{\text{C1}} - r_2 i_{\text{L2}} - L_2 \frac{di_{\text{L2}}}{dt}, \quad (8)$$

$$0 = -u_{\text{C2}} + r_2 i_{\text{L2}} + L_2 \frac{di_{\text{L2}}}{dt}, \quad (9)$$

$$0 = -R_{\mathrm{load}} i_{\mathrm{load}} + u_{\mathrm{C2}}. \quad (10)$$

For the second phase, equations for the currents flowing through capacitors C1 and C2 are determined by the following formulas:

$$-i_{\mathrm{L1}} = C_1 \frac{du_{\mathrm{C1}}}{dt}, \quad (11)$$

$$-i_{\mathrm{L2}} = C_2 \frac{du_{\mathrm{C2}}}{dt}. \quad (12)$$

Expressing $\frac{di_{\mathrm{L2}}}{dt}$ from Eq. (9) and substituting it into Eq. (8), the first two equations in Cauchy form can be obtained. Expressing $\frac{du_{\mathrm{C1}}}{dt}$ from Eq. (12) and substituting i_{load} from Eq. (7) into Eq. (10), two more equations in Cauchy form are obtained, as follows:

$$\begin{cases} \dfrac{di_{\mathrm{L1}}}{dt} = \dfrac{U_{\mathrm{in}}}{L_1} - \dfrac{r_1}{L_1} i_{\mathrm{L1}} + \dfrac{1}{L_1} u_{\mathrm{C1}} + \dfrac{1}{L_1} u_{\mathrm{C2}}, \\ \dfrac{di_{\mathrm{L2}}}{dt} = \dfrac{1}{L_2} u_{\mathrm{C2}} - \dfrac{r_2}{L_2} i_{\mathrm{L2}}, \\ \dfrac{du_{\mathrm{C1}}}{dt} = -\dfrac{1}{C_1} i_{\mathrm{L1}}, \\ \dfrac{du_{\mathrm{C2}}}{dt} = -\dfrac{1}{C_2} i_{\mathrm{L1}} - \dfrac{1}{C_2} i_{\mathrm{L2}} + \dfrac{1}{R_{\mathrm{load}} C_2} u_{\mathrm{C2}}. \end{cases} \quad (13)$$

Thus, Eqs. (13) form a system of differential equations in Cauchy form which describe the second phase of the SEPIC DC/DC converter operation.

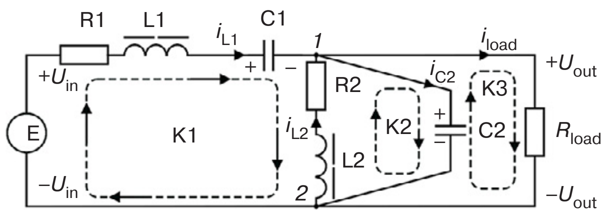

Fig. 5. Circuits on the SEPIC converter circuit operating in the energy transfer phase

TRANSFORMING SYSTEMS OF DIFFERENTIAL EQUATIONS IN CAUCHY FORM INTO MATRIX FORM TO OBTAIN A GENERALIZED MATRIX SYSTEM

For the convenient transformation of systems of differential Eqs. (6) and (13) into the generalized LCM, it would be reasonable to represent them in the form of coefficient matrices. These are multiplied by a matrix with variables in the form of currents and voltages: the so-called matrix $\mathbf{X}$ of the system phase coordinates. Therefore, each phase of the converter operation can be represented in the following form:

$$\mathbf{X} = \begin{bmatrix} i_{\mathrm{L1}} \\ i_{\mathrm{L2}} \\ u_{\mathrm{C1}} \\ u_{\mathrm{C2}} \end{bmatrix}, \quad \frac{d\mathbf{X}}{dt} = \mathbf{AX} + \mathbf{B}U, \quad (14)$$

where $\mathbf{A}$ is the coefficient matrix of phase coordinates, U is the external power supply, $\mathbf{B}$ is the coefficient matrix of the external source, and t is time.

After transformation of systems of differential Eqs. (6) and (13) into coefficient matrices $\mathbf{A}_1$, $\mathbf{B}_1$ and $\mathbf{A}_2$, $\mathbf{B}_2$, the following is obtained:

$$\mathbf{A}_1 = \begin{bmatrix} -\dfrac{r_1}{L_1} & 0 & 0 & 0 \\ 0 & -\dfrac{r_2}{L_2} & -\dfrac{1}{L_2} & 0 \\ 0 & \dfrac{1}{C_1} & 0 & 0 \\ 0 & 0 & 0 & \dfrac{1}{R_{\mathrm{load}} C_2} \end{bmatrix}, \quad (15)$$

$$\mathbf{A}_2 = \begin{bmatrix} -\dfrac{r_1}{L_1} & 0 & \dfrac{1}{L_1} & \dfrac{1}{L_1} \\ 0 & -\dfrac{r_2}{L_2} & 0 & \dfrac{1}{L_2} \\ -\dfrac{1}{C_1} & 0 & 0 & 0 \\ -\dfrac{1}{C_2} & -\dfrac{1}{C_2} & 0 & \dfrac{1}{R_{\mathrm{load}} C_2} \end{bmatrix}, \quad (16)$$

$$\mathbf{B}_1 = \begin{bmatrix} \dfrac{1}{L_1} \\ 0 \\ 0 \\ 0 \end{bmatrix}, \quad (17)$$

$$\mathbf{B}_2 = \begin{bmatrix} \dfrac{1}{L_1} \\ 0 \\ 0 \\ 0 \end{bmatrix}, \quad (18)$$

where $\mathbf{A}_1$ and $\mathbf{A}_2$ are the coefficient matrices of the phase coordinates of the first and second phase, respectively, while $\mathbf{B}_1$ and $\mathbf{B}_2$ are the coefficient matrices of the external source of the first and second phase, respectively.

The duration of the first phase of the converter operation is determined by fill factor D and is equal to DT, while the duration of the second phase is equal to $(1 - D)T$, where T is the switching period of the power switch VT1. Therefore, matrix $\mathbf{A}$ can be represented as $\mathbf{A}_1 D + \mathbf{A}_2(1 - D)$, while matrix $\mathbf{B}$ can be represented as $\mathbf{B}_1 D + \mathbf{B}_2(1 - D)$. It would thus be reasonable to combine matrices (15)–(18) into a generalized system, as follows:

$$\frac{d\mathbf{X}}{dt} = (\mathbf{A}_1 D + \mathbf{A}_2(1-D))\mathbf{X} + \\ + (\mathbf{B}_1 D + \mathbf{B}_2(1-D))U = \mathbf{A}\mathbf{X} + \mathbf{B}U.$$

Then matrices $\mathbf{A}$ and $\mathbf{B}$ can be written in the following form:

$$\mathbf{A} = \begin{bmatrix} -\frac{r_1}{L_1} & 0 & \frac{1-D}{L_1} & \frac{1-D}{L_1} \\ 0 & -\frac{r_2}{L_2} & -\frac{D}{L_2} & \frac{1-D}{L_2} \\ -\frac{1-D}{C_1} & \frac{D}{C_1} & 0 & 0 \\ -\frac{1-D}{C_2} & -\frac{1-D}{C_2} & 0 & \frac{1}{R_{\text{load}} C_2} \end{bmatrix}, \quad (19)$$

$$\mathbf{B} = \begin{bmatrix} \frac{1}{L_1} \\ 0 \\ 0 \\ 0 \end{bmatrix}. \quad (20)$$

Thus, the system of equations (14), (19), and (20) is the LCM for the DC/DC converter based on SEPIC topology.

ANALYSIS OF THE LCM

It would be advisable to start LCM analysis by defining DC currents and voltages. The voltages and currents of a real device are the sum of constant and variable components. In order to simplify the circuit analysis, it would be advisable to study the considered device in a steady state when the transient process is over. In this case, constant values of currents and voltages do not depend on time. This allows the LCM for the steady state to be written in the following form:

$$\begin{cases} -\frac{r_1}{L_1} I_{\text{L1}} + \frac{1-D}{L_1} U_{\text{C1}} + \frac{1-D}{L_1} U_{\text{C2}} = -\frac{1}{L_1} U_{\text{in}}, \\ -\frac{r_2}{L_2} I_{\text{L2}} - \frac{D}{L_2} U_{\text{C1}} + \frac{1-D}{L_2} U_{\text{C2}} = 0, \\ -\frac{1-D}{C_1} I_{\text{L1}} + \frac{D}{C_1} I_{\text{L2}} = 0, \\ -\frac{1-D}{C_2} I_{\text{L1}} - \frac{1-D}{C_2} I_{\text{L2}} - \frac{1}{R_{\text{load}} C_2} U_{\text{C2}} = 0, \end{cases} \quad (21)$$

where I_{L1}, I_{L2} are constant currents flowing through the windings of inductors L1 and L2, respectively; U_{C1}, U_{C2} are constant voltages on capacitors C1 and C2, respectively. Solving the system of equations (21), the following formulas for determining the constant currents and voltages can be obtained:

$$I_{\text{L1}} = \\ = \frac{-U_{\text{in}} D^2}{\left(D^2 - 2D + 1\right) r_2 + D^2 r_1 + (2R_{\text{load}} D - R_{\text{load}} D^2 - R_{\text{load}})}, \quad (22)$$

$$I_{\text{L2}} = \\ = \frac{U_{\text{in}} D^2 - U_{\text{in}} D}{\left(D^2 - 2D + 1\right) r_2 + D^2 r_1 + (2R_{\text{load}} D - R_{\text{load}} D^2 - R_{\text{load}})}, \quad (23)$$

$$U_{\text{C1}} = \\ = \frac{\left(-U_{\text{in}} D + U_{\text{in}}\right) r_2 + \left(2R_{\text{load}} U_{\text{in}} D - R_{\text{load}} U_{\text{in}} D^2 - R_{\text{load}} U_{\text{in}}\right)}{\left(D^2 - 2D + 1\right) r_2 + D^2 r_1 + \left(2R_{\text{load}} D - R_{\text{load}} D^2 - R_{\text{load}}\right)}, \quad (24)$$

$$U_{\text{C2}} = \\ = -\frac{R_{\text{load}} U_{\text{in}} D^2 - R_{\text{load}} U_{\text{in}} D}{\left(D^2 - 2D + 1\right) r_2 + D^2 r_1 + \left(2R_{\text{load}} D - R_{\text{load}} D^2 - R_{\text{load}}\right)}. \quad (25)$$

These equations can be substantially simplified by assuming that ohmic resistances r_1 and r_2 of the inductor windings L1 and L2 are zero. Then Eqs. (22)–(25) can be written in the following form:

$$I_{\text{L1}} = \frac{U_{\text{in}} D^2}{(D-1)^2 R_{\text{load}}}, \quad (26)$$

$$I_{\text{L2}} = \frac{U_{\text{in}} D}{(1-D) R_{\text{load}}}, \quad (27)$$

$$U_{\text{C1}} = U_{\text{in}}, \quad (28)$$

$$U_{\text{C2}} = \frac{U_{\text{in}} D}{(1-D) R_{\text{load}}}. \quad (29)$$

Equations (22)–(25) are the basis for designing the DC/DC converter based on SEPIC topology and allow the calculation of constant currents I_{L1} and I_{L2} flowing

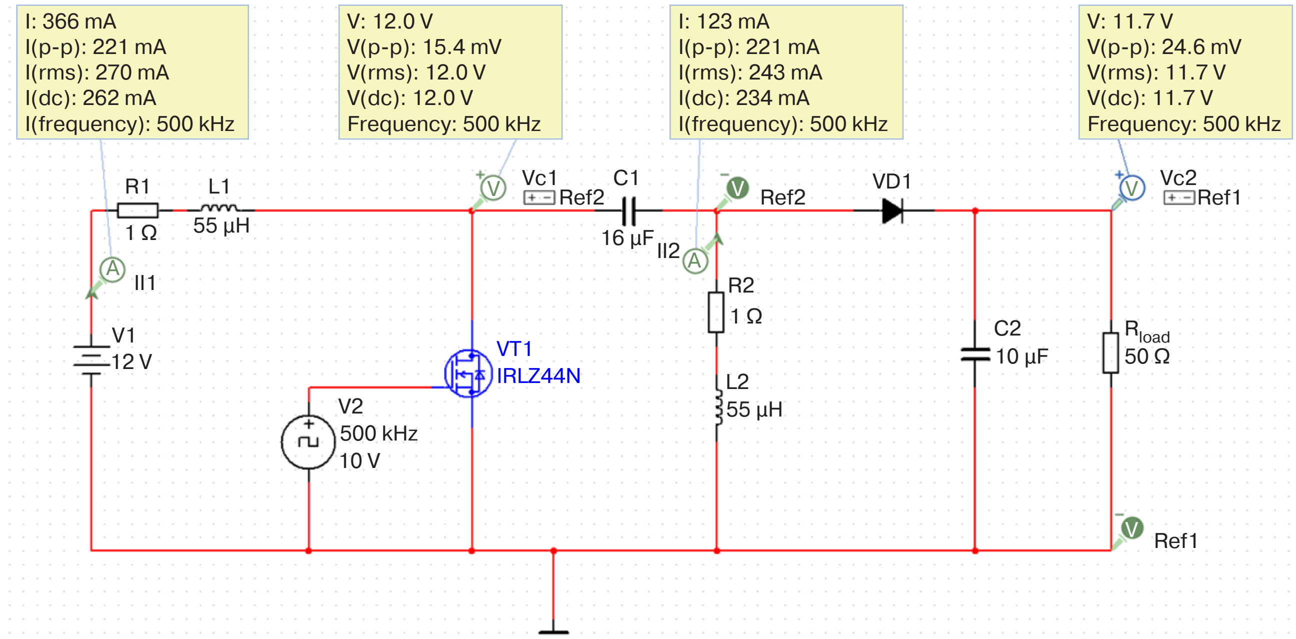

Fig. 6. Simulation circuit of the DC/DC converter based on SEPIC topology

through the windings of inductors L1 and L2, as well as voltages U_{C1} and U_{C2} on capacitors C1 and C2. Equations (26)–(29) are required for estimating the converter.

SIMULATION IN *MULTISIM*

The simulation circuit for the DC/DC converter based on SEPIC topology is shown in Fig. 6. Electronic elements are selected from *Multisim* database.[2] MOSFET IRLZ44N (International Rectifier, USA) is selected as power switch VT1. This transistor has been previously investigated in static and dynamic modes and has been compared with data from Datasheet [20, 21]. The analysis results show that the IRLZ44N transistor model in *Multisim* environment corresponds to the characteristics given in Datasheet.

The power supply is represented as the element of constant voltage V1. Modulation of the power switch VT1 is accomplished by pulse width modulation signal generator V2. The constant components of currents and voltages are measured by samples on the circuit in the DC mode. It should be noted that the measurements are carried out 3–5 ms after the start of simulation, thus enabling the currents and voltages in the steady state of the DC/DC converter under consideration to be measured.

The dependence plots of constant currents and voltages on fill factor *D* are shown in Figs. 7 and 8. There is an obvious correlation between calculated values obtained using LCM and the values obtained by simulation within the range of fill factor *D* changing from 0.3 to 0.7. It is worth noting that at fill factor *D* around 0.5, the best coincidence between calculated values and those obtained in simulation is observed.

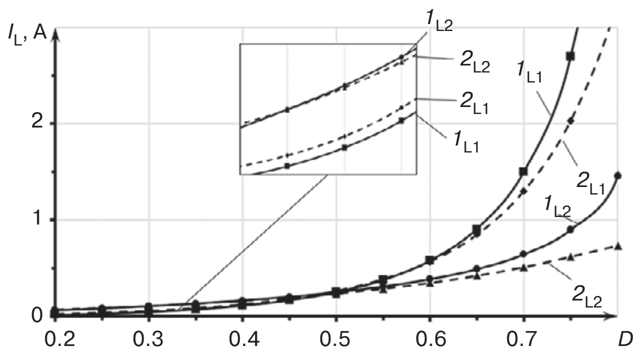

Fig. 7. Effect of the fill factor on currents flowing through the windings of inductors L1 and L2: 1_{L1} and 1_{L2} are calculation; 2_{L1} and 2_{L2} are simulation

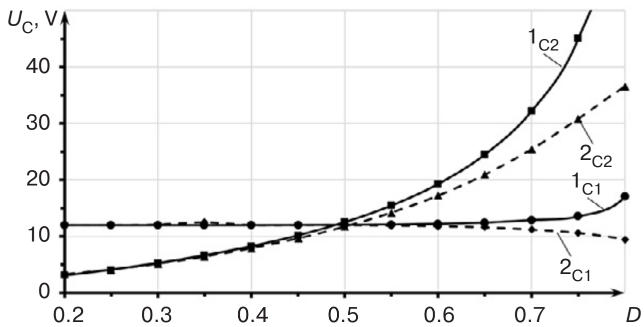

Fig. 8. Effect of fill factor on voltages on capacitors C1 and C2: 1_{C1} and 1_{C2} are calculation; 2_{C1} and 2_{C2} are simulation

[2] https://www.ni.com/en/support/downloads/software-products/download.multisim.html#452133. Accessed April 09, 2023.

At fill factor $D = 0.5$, the difference between calculated values and simulation results for currents flowing through inductor windings is 12 and 16 mA, with calculated value I_{L1} and I_{L2} equal to 250 mA. For capacitor C2 voltage, the difference between calculated values and simulation results is 0.8 V with a calculated value U_{C2} equal to 12.5 V. The calculated voltage value U_{C1} = 12.0 V coincides with the voltage obtained in simulation.

The difference between the calculated value and the value obtained in simulation for current I_{L1} at fill factor $D = 0.3$ is 11 mA, while at $D = 0.7$ it amounts to 0.2 A. The calculated current values I_{L1} are 45 mA and 1.5 A, respectively. Similarly, it may be noted that the difference of current I_{L2} is 2 mA at $D = 0.3$ and 135 mA at $D = 0.7$ for calculated current I_{L2} equal to 105 mA and 643 mA, respectively.

The difference between the calculated and simulated voltage values U_{C1} is 0.16 V at D = 0.3 and 1.65 V at D = 0.7, with the calculated value of DC voltage U_{C1} varying from 11.94 V at D = 0.3 to 12.85 V at $D = 0.7$. A similar dependence is also characteristic of the DC voltage U_{C2}. This difference is 0.13 V at calculated value $U_{C2,}$ equal to 5.27 V, and 6.75 V at calculated value U_{C2} equal to 32.1 V for $D = 0.3$ and $D = 0.7$, respectively.

Similar dependences of calculated and simulated currents and voltages are characteristic of LCM for the DC/DC converter based on Zeta topology [15–17]. The dependences of currents I_{L1}, I_{L2} and voltages U_{C1}, U_{C2} on frequency also have a similarity: the calculated values begin to correspond to the values obtained in simulation at switching frequency f of the power switch VT1 above 200 kHz only. In addition, the graphs of calculated and simulation values intersect each other in the neighborhood of fill factor D = 0.5. When the fill factor increases or decreases, the difference between the values increases.

The graphs presented in Figs. 9 and 10 show that when switching frequency f of the power transistor increases, the values of DC currents and voltages described by LCM tend towards corresponding values of DC currents and voltages obtained in simulation (as described in [15–17]). This illustrates the limitation of the mathematical model for the DC/DC converter based on SEPIC topology.

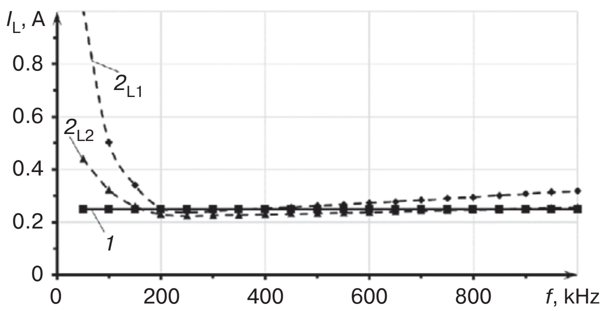

Fig. 9. Effect of switching frequency on currents flowing through the windings of the first and the second inductor at fill factor equal to 0.5: *1* is calculation; 2_{L1} and 2_{L2} are simulation

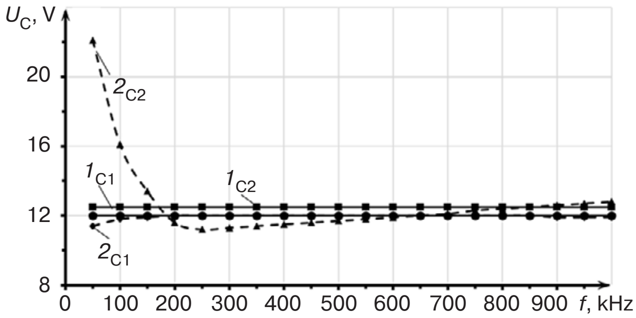

Fig. 10. Effect of switching frequency on voltages on the first and second capacitor at fill factor equal to 0.5: 1_{C1} and 1_{C2} are calculation; 2_{C1} and 2_{C2} are simulation

CONCLUSIONS

This is the first time that the LCM of the unipolar DC/DC converter based on SEPIC topology has been obtained. The analysis results of the equivalent circuits of the considered converter for both operation phases are given. Kirchhoff's rules were used to obtain differential equations for algebraic sums of currents and voltages in the device describing changes in the input power supply current, currents flowing through the windings of inductors L1 and L2, and voltages on capacitors C1 and C2.

The systems of differential equations in Cauchy form written for each phase of converter operation are transformed into coefficient matrices. This allows for the limit continuous mathematical model for DC/DC converter to be formulated. The mathematical model is used to obtain equations for calculating constant currents flowing through the inductor windings and the voltages on capacitors in the converter steady-state operation.

Calculation results using the obtained limit continuous mathematical model are compared with those obtained in the DC/DC converter simulation. Current values I_{L1} obtained in simulation differ from the calculated value in the range from 11 mA to 0.2 A. These correspond to the percentage value of 13–24%. Similarly, for current I_{L2}, the values range from 2 to 135 mA, that in percentage terms corresponds to a range of 2–20%. A similar pattern is characteristic of voltages U_{C1} and U_{C2}. The voltages deviate from the calculated value from 0.16 to 1.65 V for U_{C1} and from 0.13 to 6.74 V for U_{C2}. These ranges correspond to deviations of 1–13% for U_{C1} and 3–20% for U_{C2}. In addition, it is shown that at switching frequencies of the power switch VT1 greater than 200 kHz, there are small differences between calculated values and those obtained in simulation.

The LCM for the DC/DC converter based on SEPIC topology is the basis for its circuit design and physico-mathematical analysis.

Authors' contribution. All authors equally contributed to the research work.

REFERENCES

1. Vasyukov I.V., Pavlenko A.V., Batishchev D.V. Review and Analysis of Topologies of Converters of Power Supply Systems on Hydrogen Fuel Cells for Unmanned Aerial Vehicles of Kilowatt Power Class. *Izvestiya vysshikh uchebnykh zavedenii. Elektromekhanika = Russian Electromechanics*. 2022;65(2):19–26 (in Russ.). https://doi.org/10.17213/0136-3360-2022-2-19-26
2. Antchev H., Andonov A. Simple PV battery charger without MPPT based on SEPIC converter. *Electrotechnica & Electronica* (*E+E*). 2019;54(3–4):64–69. Available from URL: https://epluse.ceec.bg/wp-content/uploads/2019/08/20190304-04.pdf
3. Kushwaha R., Singh B. UPF-isolated zeta converter-based battery charger for electric vehicle. *IET Electrical Systems in Transportation*. 2019;9(3):103–112. https://doi.org/10.1049/iet-est.2018.5010
4. Sharov I.M., Demin O.A., Sudakov A.A., Yarlykov A.D. Development and research of an uninterruptible power supply system in networks with voltage up to 24 V. *Russ. Technol. J.* 2022;10(5):60–72 (in Russ.). https://doi.org/10.32362/2500-316X-2022-10-5-60-72
5. Murthy-Bellur D., Kazimierczuk M.K. Two-transistor Zeta-flyback DC-DC converter with reduced transistor voltage stress. *Electron. Lett*. 2010;46(10):719–720. https://doi.org/10.1049/el.2010.3494
6. Thirumeni M., Thangavelusamy D. Performance analysis of PI and SMC controlled zeta converter. *Int. J. Recent Technol. Eng*. 2019;8(3):8700–8706. http://www.doi.org/10.35940/ijrte.C5242.098319
7. Erickson R.W., Maksimović D. *Fundamentals of Power Electronics*. NY: Springer; 2020. 1084 p. https://doi.org/10.1007/978-3-030-43881-4
8. Korshunov A.I. Limiting continuous model of a system with high-frequency structure variation. *Izvestiya vysshikh uchebnykh zavedenii. Priborostroenie = J. Instrument Eng.* 2009;52(9):42–48 (in Russ.). Available from URL: https://pribor.ifmo.ru/file/article/4902.pdf
9. Korshunov A.I. Limiting Continuous Model of System with High-Frequency Variable Structure. *Silovaya elektronika.* 2021;5(92):48–51 (in Russ.).
10. Korshunov A.I. Methodology for constructing continuous models of pulsed DC voltage converters. *Komponenty i tekhnologii = Components & Technologies*. 2006;8(61):124–130 (in Russ.). Available from URL: https://kit-e.ru/powerel/metodika-postroeniya-nepreryvnyh-modelej-impulsnyh-preobrazovatelej-napryazheniya-postoyannogo-toka/
11. Korshunov A.I. Improving the quality of output voltage stabilisation of a pulsed DC converter. *Izvestiya vysshikh uchebnykh zavedenii. Priborostroenie = J. Instrument Eng.* 2013;56(3):48–57 (in Russ.). Available from URL: https://pribor.ifmo.ru/file/article/6176.pdf
12. Korshunov A.I. Two approaches to stability analysis of DC-DC converters with variable structure of power stage. *Prakticheskaya silovaya elektronika = Practical Power Electronics*. 2017;2(66):12–19 (in Russ.).
13. Korshunov A.I. Pulsed DC voltage converter based on Chuk scheme. *Silovaya elektronika = Power Electronics*. 2017;4(67):60–66 (in Russ.).
14. Korshunov A.I. Specifics of DC voltage stabilization by Chuk converter. *Prakticheskaya silovaya elektronika = Practical Power Electronics*. 2017;4(68):2–9 (in Russ.).
15. Bityukov V.K., Lavrenov A.I., Malitskiy D.A. Mathematical model of DC/DC converter based on Zeta topology (Part 1). *Proektirovanie i tekhnologiya elektronnykh sredstv = Design and Technology of Electronic Means*. 2022;4:53–57 (in Russ.).
16. Bityukov V.K., Lavrenov A.I., Malitskiy D.A. Mathematical model of DC/DC converter based on Zeta topology (Part 2). *Proektirovanie i tekhnologiya elektronnykh sredstv = Design and Technology of Electronic Means*. 2023;1:48–53 (in Russ.).
17. Bityukov V.K., Lavrenov A.I., Malitskiy D.A. Analysis of the DC/DC Zeta topology converter ripples by applying its limiting continuous mathematical model. *Russ. Technol. J.* 2023;11(4):36–48 (in Russ.). https://doi.org/10.32362/2500-316X-2023-11-4-36-48
18. Odinokov A.O., Kremzukov Yu.A. Selecting DC converter topology. SEPIC or Zeta. *Prakticheskaya silovaya elektronika = Practical Power Electronics*. 2022;4(88):44–47 (in Russ.).
19. Bityukov V.K., Simachkov D.S., Babenko V.P. *Skhemotekhnika elektropreobrazovatel'nykh ustroistv* (*Circuitry of Electrical Converter Devices*). Vologda: Infra-Inzheneriya; 2023. 384 p. (in Russ.). ISBN 978-5-9729-1439-5
20. Babenko V.P., Bityukov V.K. Simulation of Switching of High-Power FETs Using the Electronics Workbench Software. *J. Commun. Technol. Electron.* 2019;64(2):176–181. https://doi.org/10.1134/S1064226919020025
    [Original Russian Text: Babenko V.P., Bityukov V.K. Simulation of Switching of High-Power FETs Using the Electronics Workbench Software. *Radiotekhnika i Elektronika.* 2019;64(2):199–205 (in Russ.). https://doi.org/10.1134/S0033849419020025]
21. Babenko V.P., Bityukov V.K., Kuznetsov V.V., Simachkov D.S. Simulation of static and dynamic losses in MOSFET keys. *Russ. Technol. J*. 2018;6(1):20–39 (in Russ.). Available from URL: https://doi.org/10.32362/2500-316X-2018-6-1-20-39

СПИСОК ЛИТЕРАТУРЫ

1. Васюков И.В., Павленко А.В., Батищев Д.В. Обзор и анализ топологий преобразователей систем электропитания на водородных топливных элементах для беспилотных летательных аппаратов киловаттного класса мощности. *Известия вузов. Электромеханика*. 2022;65(2):19–26. https://doi.org/10.17213/0136-3360-2022-2-19-26

2. Antchev H., Andonov A. Simple PV battery charger without MPPT based on SEPIC converter. *Electrotechnica & Electronica* (*E+E*). 2019;54(3–4):64–69. URL: https://epluse.ceec.bg/wp-content/uploads/2019/08/20190304-04.pdf
3. Kushwaha R., Singh B. UPF-isolated zeta converter-based battery charger for electric vehicle. *IET Electrical Systems in Transportation*. 2019;9(3):103–112. https://doi.org/10.1049/iet-est.2018.5010
4. Шаров И.М., Демин О.А., Судаков А.А., Ярлыков А.Д. Разработка и исследование системы бесперебойного питания в сетях с напряжением до 24 В. *Russ. Technol. J*. 2022;10(5):60–72. https://doi.org/10.32362/2500-316X-2022-10-5-60-72
5. Murthy-Bellur D., Kazimierczuk M.K. Two-transistor Zeta-flyback DC-DC converter with reduced transistor voltage stress. *Electron. Lett*. 2010;46(10):719–720. https://doi.org/10.1049/el.2010.3494
6. Thirumeni M., Thangavelusamy D. Performance analysis of PI and SMC controlled zeta converter. *Int. J. Recent Technol. Eng*. 2019;8(3):8700–8706. http://www.doi.org/10.35940/ijrte.C5242.098319
7. Erickson R.W., Maksimović D. *Fundamentals of Power Electronics*. NY: Springer; 2020. 1084 p. https://doi.org/10.1007/978-3-030-43881-4
8. Коршунов А.И. Предельная непрерывная модель системы с высокочастотным периодическим изменением структуры. *Известия вузов. Приборостроение*. 2009;52(9):42–48. URL: https://pribor.ifmo.ru/file/article/4902.pdf
9. Коршунов А.И. Предельная непрерывная модель системы с периодическим высокочастотным изменением структуры. *Силовая электроника*. 2021;5(92):48–51.
10. Коршунов А.И. Методика построения непрерывных моделей импульсных преобразователей напряжения постоянного тока. *Компоненты и технологии*. 2006;8(61):124–130. URL: https://kit-e.ru/powerel/metodika-postroeniya-nepreryvnyh-modelej-impulsnyh-preobrazovatelej-napryazheniya-postoyannogo-toka/
11. Коршунов А.И. Повышение качества стабилизации выходного напряжения импульсного преобразователя постоянного тока. *Известия вузов. Приборостроение*. 2013;56(3):48–57. URL: https://pribor.ifmo.ru/file/article/6176.pdf
12. Коршунов А.И. Два подхода к анализу устойчивости стабилизаторов напряжения постоянного тока с переменной структурой силовой части. *Практическая силовая электроника*. 2017;66:12–19.
13. Коршунов А.И. Импульсный преобразователь напряжения постоянного тока по схеме Чука. *Силовая электроника*. 2017;4(67):60–66.
14. Коршунов А.И. Особенности стабилизации напряжения постоянного тока с помощью преобразователя Чука. *Практическая силовая электроника*. 2017;4(68):2–9.
15. Битюков В.К., Лавренов А.И., Малицкий Д.А. Математическая модель DC/DC преобразователя, построенного по Zeta топологии (часть 1). *Проектирование и технология электронных средств*. 2022;4:53–57.
16. Битюков В.К., Лавренов А.И., Малицкий Д.А. Математическая модель DC/DC преобразователя, построенного по Zeta топологии (часть 2). *Проектирование и технология электронных средств*. 2023;1:48–53.
17. Битюков В.К., Лавренов А.И., Малицкий Д.А. Анализ пульсаций DC/DC преобразователя, построенного по Zeta топологии, с использованием его предельной непрерывной математической модели. *Russ. Technol. J.* 2023;11(4):36–48. https://doi.org/10.32362/2500-316X-2023-11-4-36-48
18. Одиноков А.О., Кремзуков Ю.А. Выбор топологии преобразователя постоянного напряжения. SEPIC или Zeta. *Практическая силовая электроника*. 2022;4(88):44–47.
19. Битюков В.К., Симачков Д.С., Бабенко В.П. *Схемотехника электропреобразовательных устройств*. Вологда: Инфра-Инженерия; 2023. 384 с. ISBN 978-5-9729-1439-5
20. Бабенко В.П., Битюков В.К. Имитационное моделирование процессов переключения силовых полевых транзисторов в программе Electronics Workbench. *Радиотехника и электроника*. 2019;64(2):199–205. https://doi.org/10.1134/S0033849419020025
21. Бабенко В.П., Битюков В.К., Кузнецов В.В., Симачков Д.С. Моделирование статических и динамических потерь в MOSFET ключах. *Российский технологический журнал.* 2018;6(1):20–39. https://doi.org/10.32362/2500-316X-2018-6-1-20-39

About the authors

Aleksey I. Lavrenov, Assistant, Department of Radio Wave Processes and Technology, Institute of Radio Electronics and Informatics, MIREA – Russian Technological University (78, Vernadskogo pr., Moscow, 119454 Russia). E-mail: lavrenov@mirea.ru. RSCI SPIN-code 6048-5027, https://orcid.org/0000-0001-5722-541X

Vladimir K. Bityukov, Dr. Sci. (Eng.), Professor, Department of Radio Wave Processes and Technologies, Institute of Radio Electronics and Informatics, MIREA – Russian Technological University (78, Vernadskogo pr., Moscow, 119454 Russia). E-mail: bitukov@mirea.ru. ResearcherID Y-8325-2018, Scopus Author ID 6603797260, RSCI SPIN-code 3834-5360, https://orcid.org/0000-0001-6448-8509

Об авторах

Лавренов Алексей Игоревич, ассистент, кафедра радиоволновых процессов и технологий Института радиоэлектроники и информатики ФГБОУ ВО «МИРЭА – Российский технологический университет» (119454, Россия, Москва, пр-т Вернадского, д. 78). E-mail: lavrenov@mirea.ru. SPIN-код РИНЦ 6048-5027, https://orcid.org/0000-0001-5722-541X

Битюков Владимир Ксенофонтович, д.т.н., профессор, профессор кафедры радиоволновых процессов и технологий Института радиоэлектроники и информатики ФГБОУ ВО «МИРЭА – Российский технологический университет» (119454, Россия, Москва, пр-т Вернадского, д. 78). E-mail: bitukov@mirea.ru. ResearcherID Y-8325-2018, Scopus Author ID 6603797260, SPIN-код РИНЦ 3834-5360, https://orcid.org/0000-0001-6448-8509

Translated from Russian into English by Kirill V. Nazarov
Edited for English language and spelling by Dr. David Mossop